We are IntechOpen,
the world's leading publisher of
Open Access books
Built by scientists, for scientists

6,900
Open access books available

185,000
International authors and editors

200M
Downloads

Our authors are among the

154
Countries delivered to

TOP 1%
most cited scientists

12.2%
Contributors from top 500 universities

CLARIVATE ANALYTICS

BOOK
CITATION
INDEX

INDEXED

WEB OF SCIENCE™

Selection of our books indexed in the Book Citation Index
in Web of Science™ Core Collection (BKCI)

Interested in publishing with us?
Contact book.department@intechopen.com

Numbers displayed above are based on latest data collected.
For more information visit www.intechopen.com

Exact and Asymptotic Analysis of Largest Eigenvalue Based Spectrum Sensing

Olav Tirkkonen and Lu Wei
Aalto University
Finland

1. Introduction

Cognitive radio (CR) is a promising technique for future wireless communication systems. In CR networks, dynamic spectrum access (DSA) of frequency is implemented to mitigate spectrum scarcity. Specifically, a secondary (unlicensed) user may be allowed to access the temporarily unused frequency bands granted to a primary (licensed) user. DSA has to be implemented so that the quality of service (QoS) promised to the primary user must be satisfied. The key point for this is the secondary user's ability to detect the presence of the primary user correctly. Therefore a quick and reliable spectrum occupancy decision based on spectrum sensing becomes a critical issue irrespective of the architecture of the CR networks.

Several spectrum sensing methods exist in the literature. Energy detection has been considered in (Digham et al., 2003; Sahai & Cabric, 2005; Tandra & Sahai, 2005), matched filter detection in (Kay, 1993), cyclostationary feature detection in (Gardner, 1991). Recently, eigenvalue based detection has been proposed in (Penna et al., 2009A;B; Penna & Garello, 2010; Wei & Tirkkonen, 2009; Zeng et al., 2008; Zeng & Liang, 2008). Each of these techniques has its strengths and weaknesses. For example, matched filter detection and cyclostationary feature detection require knowledge on the waveform of the primary user, which is impractical for certain applications. Energy detection and eigenvalue based detection are so-called blind detection methods which do not need any a priori information of the signal. Eigenvalue based detection can be further divided into eigenvalue ratio based (ER) detectors and largest eigenvalue based (LE) detectors. The ER detection circumvents the need to know the noise power, since asymptotically its test statistics does not depend on the noise power. Noise uncertainty (Tandra & Sahai, 2005) may has important consequences for detector performance. For example, ER outperforms energy detector, when there is uncertainty of the noise level. In the literature, performance analysis of the ER detector relies on the limiting laws of the largest and the smallest eigenvalue distributions. These limiting laws are valid for large numbers of sensors and samples and are not able to characterize detection performance when the number of sensors and the sample size are small. On the other hand, exact characterization of the ER detection requires knowledge of the condition number distribution of finite dimensional covariance matrices, which is generically mathematically intractable. A semi-analytical expression of the condition number distribution is presented in (Penna et al., 2009A). This result becomes rather complicated to implement when the number of sensors and the sample sizes are large. For the LE detector, asymptotical performance analysis based on the Tracy-Widom distribution is proposed in (Zeng et al., 2008). There, the limiting law of the

largest eigenvalue distribution is utilized to set a decision threshold, considering only the false alarm probability. This result characterizes the LE detector performance in the asymptotical region where the sample sizes and the number of cooperating sensors are huge. In (Kritchman & Nadler, 2009) a more general problem of estimating the number of signals using the largest eigenvalue is studied, where the estimation probability is obtained using the Tracy-Widom distribution as well. Finally we note that the LE detector is similar to the energy detector in that the test statistics are functions of the noise variance. Therefore the LE detector is pestered by the noise uncertainty problem as well.

In this chapter, the analysis of eigenvalue detector is carried out in a setting where there is only one primary user transmitting. The detection problem is a hypothesis test between two possible hypotheses; either there is a primary user, or there is none. The covariance matrices under these hypotheses can be formulated as central and non-central Wishart matrices, respectively. Empirically we found that the largest eigenvalue calculated from the received covariance matrix is an efficient quantity to discriminate between the two hypotheses, which motivates the investigation of the LE detection.

The contribution of this chapter is two-fold. Firstly we derive the exact largest eigenvalue distributions for central and non-central Wishart matrices. We modify the results on the largest eigenvalue distributions from (Dighe et al., 2003; Kang & Alouini, 2003; Khatri, 1964) in order to derive distribution functions suitable for performance analysis. As a result we obtain exact characterizations for both the false alarm probability and the probability of missed detection. Secondly, we investigate the detection performance in the asymptotical region where both the number of sensors and the sample size are large. Specifically we derive closed-form asymptotic largest eigenvalue distributions for central and non-central Wishart matrices. These results are possible due to recent breakthrough in random matrix theory. Moreover a simple closed-form formula for the receiver operating characteristics (ROC) can also be derived. Besides gaining more insights into the detection performance, the low complexity asymptotic results can be used for the implementation of the LE detector.

The accuracy of the asymptotic approximations is investigated by comparing to the exact distributions through various realistic spectrum sensing scenarios. The results confirm the usefulness of the asymptotic distributions in analyzing the detection performance in practice. We also compare the detection performance of the LE detection with other well-known detection schemes. It turns out that in the case of perfectly estimated noise power the LE detector performs best among the detectors considered. In order to see the whole picture, we extend the analysis to the case where the noise power is not perfectly known. With worst case noise uncertainty, the LE detector performs worse than the ER detector, but is by far more robust against noise uncertainty the energy detector.

The rest of this chapter is organized as follows. In Section 2, we formulate the primary user detection problem in a multi-antenna spectrum sensing setting. We then motivate the choice of largest eigenvalue as the test statistics. Section 3 is devoted to deriving the exact as well as the asymptotical largest eigenvalue distributions. In Section 4, we first study the impact of approximation accuracy of the asymptotic distributions on the detection performance. We then compare the detection performance of the LE detector with that of other detection methods. Lastly, we investigate the impact of the noise uncertainty on the detection performance. Finally in Section 5 we conclude the main results of this chapter.

2. Problem formulation

2.1 Signal model

Consider a primary signal detection problem with K collaborating sensors. These sensors may be, for example, K receive antennas in one secondary terminal or K collaborating secondary devices each with a single antenna, or any combination of these. We assume periodical sensing, where each sensor periodically collects N samples during a sensing time. This collaborative sensing scenario is more relevant if the K sensors are in one device, i.e. for multi-antenna assisted spectrum sensing. For multiple collaborating devices, communication to the fusion center by sensors of different locations becomes a problem even for a small sample size N.

The received $K \times N$ data matrix $\mathbf{Y}$ is represented as

$$\mathbf{Y} = \begin{pmatrix} y_{1,1} & y_{1,2} & \cdots & y_{1,N} \\ y_{2,1} & y_{2,2} & \cdots & y_{2,N} \\ \vdots & \vdots & \ddots & \vdots \\ y_{K,1} & y_{K,2} & \cdots & y_{K,N} \end{pmatrix}. \tag{1}$$

Mathematically, the primary user detection problem is a hypothesis test between two hypotheses. Hypothesis 0 ($\mathbf{H_0}$) denotes the absence of the primary user and hypothesis 1 ($\mathbf{H_1}$) denotes the presence of the primary user. If we assume no fading in the temporal domain, i.e. the channel stays constant during the sensing time, the two hypotheses can be represented as:

$$\mathbf{H_0} : y_{k,n} = n_{k,n} \tag{2}$$

$$\mathbf{H_1} : y_{k,n} = \sum_{i=1}^{P} h_k^{(i)} s_n^{(i)} + n_{k,n}, \tag{3}$$

where $k = 1, \ldots, K$ and $n = 1, \ldots, N$. Here $n_{k,n}$ is the complex Gaussian noise with zero mean and variance σ_{cn}^2, P denotes the number of simultaneously transmitting primary users. The receive covariance matrix $\mathbf{R}$ is defined as $\mathbf{R} = \mathbf{YY}^H$, where H denotes the Hermitian conjugate operator. Throughout this chapter, we make the following assumption.

Assumption: There is at most one primary user transmitting ($P = 1$), and its signal amplitude is drawn independently from a Gaussian process for every sample.

Under hypothesis $\mathbf{H_0}$, the receive covariance matrix $\mathbf{R}$ follows the complex central Wishart distribution, denoted as (Gupta, 2000) $\mathbf{R} \sim \mathcal{W}_K \left(N, \sigma_{cn}^2 \mathbf{I}_K \right)$, where $\mathbf{I}_K$ denotes the identity matrix of dimension K. Under hypothesis $\mathbf{H_1}$, by our assumption the covariance $\mathbf{R}$ follows the complex non-central Wishart distribution, which is denoted as (Gupta, 2000) $\mathbf{R} \sim \mathcal{W}_K \left(N, \sigma_{cn}^2 \mathbf{I}_K, \mathbf{MM}^H \right)$. Here $\mathbf{MM}^H$ is the non-centrality parameter matrix with $\mathbf{M} = \mathbf{h}_k^{(1)} (\mathbf{s}_n^{(1)})^T$. The complex vectors $\mathbf{h}_k^{(1)} = [h_1^{(1)}, h_2^{(1)}, \ldots, h_K^{(1)}]'$ and $\mathbf{s}_n^{(1)} = [s_1^{(1)}, s_2^{(1)}, \ldots, s_N^{(1)}]'$ are column vectors. From the assumption that there is one primary user, it follows that the matrix $\mathbf{M}$ is rank one, because $\mathrm{Rank}\,(\mathbf{M}) = \mathrm{Rank}\,(\mathbf{MM}^H) = \mathrm{Rank}\left(||\mathbf{s}^{(1)}||^2 \mathbf{h}_k^{(1)} (\mathbf{h}_k^{(1)})^H \right) = 1$. In other words, the Hermitian matrix $\mathbf{MM}^H$ has only one non-zero eigenvalue, which we denote by ϕ_1.

Strictly speaking the non-centrality parameter $\mathbf{MM}^H$ is not a constant matrix, since the norm of the transmit signal $||\mathbf{s}^{(1)}||^2$ is still a random variable. However, the randomness in $||\mathbf{s}^{(1)}||^2$ is diminishing very fast as the sample size N increases and $||\mathbf{s}^{(1)}||^2/N$ can be well approximated by the signal variance σ_s^2 for sufficiently large N. On the other hand, if we assume the primary user's signal $s_n^{(i)}$ is of constant modulus, for example, MPSK modulation, the non-centrality parameter matrix is a strictly constant matrix. We note that under $\mathbf{H_1}$ it is also possible to model $\mathbf{R}$ as the so-called spike correlation model (Penna & Garello, 2010). Whilst the spike correlation model is mathematically more tractable, it is formally valid only for Gaussian signals. Finally, the average SNR under hypothesis $\mathbf{H_1}$ is defined as SNR $= \frac{\sigma_s^2 \sigma_h^2}{\sigma_{cn}^2}$. In practice, σ_s^2 can be estimated by $||\mathbf{s}^{(1)}||^2/N$.

2.2 Test statistics

We want to discriminate between the two hypotheses based on the eigenvalues $\lambda_1 \geq \lambda_2 \geq \ldots \geq \lambda_K$ of the observed covariance matrix $\mathbf{R}$. The fact that $\mathbf{M}$ is of rank one leads to a major difference on the numerical value of the largest eigenvalue λ_1, but the impact on other eigenvalues is much smaller. This fact is firstly explored and studied in the statistics literature, where it is known as Roy's largest root test (Roy, 1953). No explicit expression for its distribution is given in (Roy, 1953). To motivate this approach, in Table 1 we empirically calculated the sample mean of the ordered eigenvalues of the covariance matrix $\mathbf{R}$ under both hypotheses, where we set the parameters $K = 4$, $N = 30$, SNR $= -5$ dB and $\sigma_{cn}^2 = 1$. From Table 1 we can see that the largest eigenvalue λ_1 provides a most prominent candidate to discriminate $\mathbf{H_0}$ from $\mathbf{H_1}$. Specifically in this case, the difference between the mean values of the largest eigenvalues can be as large as 28.447, whereas the difference between the mean values of the smallest eigenvalues is only 1.587.

$K = 4, N = 30$	λ_1	λ_2	λ_3	λ_4
$\mathbf{H_1}$(SNR = -5 dB)	73.215	38.385	27.523	18.820
$\mathbf{H_0}$	44.768	33.265	24.747	17.233

Table 1. Sample mean of the ordered eigenvalues under both hypotheses.

Using the received data matrix (1), several other sensing algorithms can be proposed. For example, the test statistics T_{ED} of the energy detector relies on the norm of the data matrix, i.e. $||\mathbf{X}||_F^2$ (Digham et al., 2003). The test statistics of the eigenvalue ratio based detector (Penna et al., 2009A;B; Penna & Garello, 2010; Zeng & Liang, 2008) is defined as $T_{\mathrm{ER}} = \lambda_1/\lambda_K$, which is the condition number of Wishart matrices.

For detection, a test variable is calculated, which is compared with its corresponding precalculated decision threshold γ to decide the presence or absence of a primary user. If $T < \gamma$ the detector chooses $\mathbf{H_0}$, otherwise $\mathbf{H_1}$ is chosen. In order to calculate the decision thresholds we need to know the distributions of the respective test statistics. For the energy detector, the test statistics under $\mathbf{H_0}$ follows a central Chi-square distribution and under $\mathbf{H_1}$ it follows a non-central Chi-square distribution (Digham et al., 2003). For the ER detector, asymptotical condition number distributions under both hypotheses are derived in (Penna et al., 2009B; Penna & Garello, 2010; Zeng & Liang, 2008). Moreover under $\mathbf{H_0}$, the exact condition number distribution can be calculated (Penna et al., 2009A). For the LE detector, asymptotical method for computing the test statistics distribution under $\mathbf{H_0}$ is presented in (Zeng et al., 2008). However, the resulting distribution can only be evaluated numerically. In

the next section, we will derive exact largest eigenvalue distributions as well as closed-form asymptotical largest eigenvalue distributions for both hypotheses.

3. The Test statistics distributions under both hypotheses

In order to analyze the detection performance of the LE detector we need to know the distributions of the largest eigenvalue under both hypotheses. In this section, we first derive the exact distributions of the largest eigenvalue by making use of finite dimensional results on Wishart matrices. The exact distributions can be utilized to calculate detection performance metrics, such as the false alarm probability, the missed detection probability or the decision threshold. On the other hand, due to the complexity of the exact results, they are most useful when the number of sensors and sample size are small. In order to characterize the detection performance in the asymptotical region where both the number of sensors and sample sizes are large, we derive asymptotic largest eigenvalue distributions under both hypotheses. Specifically by exploring recent results in random matrix theory, we derive analytical Gaussian approximations to the largest eigenvalue distributions of central and non-central Wishart matrices. The derived closed-form asymptotical distributions provide accurate approximations in realistic spectrum sensing scenarios. Due to the simplicity of the asymptotic results, computation of various performance metrics of the LE detector can be easily performed on-line.

3.1 Exact characterizations

For the signal model in the last section, computable closed-form expressions for the largest eigenvalue distributions of central and non-central (non-central matrix $\mathbf{M}$ being rank one) Wishart matrices can be derived from the results in (Kang & Alouini, 2003; Khatri, 1964). Specifically, assuming independent and identically distributed (i.i.d) entries in the received data matrices $\mathbf{Y}$ for both hypotheses, the matrix variate distribution of $\mathbf{Y}$ under $\mathbf{H_0}$ is

$$\mathbf{Y} \sim \frac{1}{\pi^{KN} \left(\sigma_{cn}^2\right)^{KN}} e^{-\text{tr}\{\mathbf{YY}^H\}/\sigma_{cn}^2}. \tag{4}$$

The corresponding Wishart distribution $\mathbf{R} = \mathbf{YY}^H$ can be trivially derived from Theorem 3.2.2 in (Gupta, 2000) by placing σ_{cn}^2 in appropriate equations. Then the joint eigenvalue distribution of the covariance matrix $\mathbf{R}$ is derived by using the result in (James, 1964). Finally, following steps in (Khatri, 1964) the cumulative distribution function (CDF) of the largest eigenvalue of the covariance matrix $\mathbf{R}$, denoted by $F_c(x\,|\sigma_{cn}^2)$, is derived as

$$F_c\left(x\,|\sigma_{cn}^2\right) = \frac{\det \mathbf{A}}{\left(\sigma_{cn}^2\right)^{KN} \prod_{k=1}^K \Gamma(N-k+1)\Gamma(K-k+1)} \tag{5}$$

where $\det(\cdot)$ denotes the matrix determinant operator and $\Gamma(\cdot)$ is the Gamma function. The i,j th entry of matrix $\mathbf{A}$ $(K \times K)$ is defined through the regularized incomplete Gamma function $\gamma_R(\cdot, \cdot)$ as $\mathbf{A}_{i,j} = (\sigma_{cn}^2)^{N-K+i+j-1}\Gamma(N-k+i+j-1)\gamma_R\left(N-K+i+j-1, \frac{x}{\sigma_{cn}^2}\right)$. When $\sigma_{cn}^2 = 1$, the above result reduces to the result in(Khatri, 1964). By elementary manipulations, $F_c\left(x\,|\sigma_{cn}^2\right)$ can be simplified to

$$F_c\left(x\,|\sigma_{cn}^2\right) = |\det \widehat{\mathbf{A}}|, \tag{6}$$

with $\widehat{\mathbf{A}}_{i,j} = \binom{N-j+i-1}{i-1} \gamma_R(N+i-j, \frac{x}{\sigma_{cn}^2})$.

Under $\mathbf{H_1}$, the matrix variate distribution of $\mathbf{Y}$ is

$$\mathbf{Y} \sim \frac{1}{\pi^{KN} \left(\sigma_{cn}^2\right)^{KN}} e^{-\text{tr}\{(\mathbf{Y}-\mathbf{M})(\mathbf{Y}-\mathbf{M})^H\}/\sigma_{cn}^2}. \tag{7}$$

The corresponding Wishart form distribution $\mathbf{R} = \mathbf{Y}\mathbf{Y}^H$ can directly be obtained from Theorem 3.5.1 in (Gupta, 2000) by placing σ_{cn}^2 in appropriate lines. The corresponding joint eigenvalue distribution of the covariance matrix $\mathbf{R}$ is derived from (James, 1964). When matrix $\mathbf{M}$ is rank one, the CDF of the largest eigenvalue of the covariance matrix $\mathbf{R}$, denoted $F_{nc}(x \,|\sigma_{cn}^2)$, can be calculated by following the derivations in (Kang & Alouini, 2003) as

$$F_{nc}\left(x \,|\sigma_{cn}^2\right) = \frac{\left(\prod_{k=1}^{K-1} \Gamma(N-k)\Gamma(K-k)\right)^{-1} \det \mathbf{B}}{e^{\frac{\phi_1}{\sigma_{cn}^2}} \left(\sigma_{cn}^2\right)^{(KN-2K+2)} \phi_1^{K-1} \Gamma(N-K+1)} \tag{8}$$

where elements in the first column of $\mathbf{B}$ are $\mathbf{B}_{i,1} = \int_0^x \beta^{N-i} e^{-\frac{\beta}{\sigma_{cn}^2}} {}_0F_1\left(N-K+1; \frac{\phi_1\beta}{\sigma_{cn}^4}\right) d\beta$ and in the second to Kth column
$\mathbf{B}_{i,j} = (\sigma_{cn}^2)^{N+K-i-j+1} \Gamma(N+K-i-j+1)\gamma_R\left(N+K-i-j+1, \frac{x}{\sigma_{cn}^2}\right), \ j = 2,\dots,N$. Here, ${}_0F_1(\cdot;\cdot)$ is the hypergeometric function of Bessel type. Recall that ϕ_1 is the only non-zero eigenvalue of the Hermitian matrix $\mathbf{M}\mathbf{M}^H$. When $\sigma_{cn}^2 = 1$, the result above reduces to the result in (Kang & Alouini, 2003). After some manipulations, $F_{nc}\left(x \,|\sigma_{cn}^2\right)$ can be simplified to

$$F_{nc}\left(x \,|\sigma_{cn}^2\right) = |\det \widehat{\mathbf{B}}|, \tag{9}$$

with elements in the first column $\widehat{\mathbf{B}}_{i,1} = \frac{\Gamma(K)}{(N-K)\Gamma(N-i)} \int_0^{x/\sigma_{cn}^2} \beta^{N-i} e^{-\beta} {}_0F_1\left(N-K+1; \frac{\phi_1\beta}{\sigma_{cn}^2}\right) d\beta$ and in the other $K-1$ columns $\widehat{\mathbf{B}}_{i,j} = \binom{N-i+j-2}{j-1} \gamma_R(N-i+j-1, \frac{x}{\sigma_{cn}^2}), \ j = 2,\dots,N$.

Based on distribution of the test statistics under $\mathbf{H_0}$, for a given threshold γ, the false alarm probability can be calculated as

$$P_{fa}(\gamma) = 1 - F_c\left(\gamma \,|\sigma_{cn}^2\right). \tag{10}$$

Similarly, for a given SNR and threshold, the missed detection probability can be obtained by using the distribution under $\mathbf{H_1}$ as

$$P_m(\gamma) = F_{nc}\left(\gamma \,|\sigma_{cn}^2\right). \tag{11}$$

Equivalently, for a target false alarm probability or missed detection probability the resulting threshold can be calculated by numerically inverting (10) or (11).

Assuming a worst case SNR, a performance bound can be obtained by the analysis above. This worst case SNR value can, for example, be set based on the receiver sensitivity of the primary system of interest (Ruttik et al., 2009). Notice that the actual detection performance could be better or worse depending on the validity of the assumed worst case SNR value. When taking into account the test statistics distributions under both hypotheses, the decision threshold can

be obtained by the Neyman-Pearson criterion (Kay, 1993) or by minimizing a weighted sum of the false alarm probability and the missed detection probability (Wei & Tirkkonen, 2009). Once we obtain the decision threshold the detection procedure is as follows. Firstly, the K cooperative sensors form the $K \times N$ received data matrix $\mathbf{Y}$ as in (1). Secondly, the largest eigenvalue λ_1 of the covariance matrix $\mathbf{R} = \mathbf{Y}\mathbf{Y}^H$ is calculated. Finally, we make a decision; if λ_1 is larger than the threshold γ it is decided that the primary user is present and if λ_1 is smaller than γ it is decided that the primary user is absent.

3.2 Asymptotical characterizations

Although the previous derived results could capture the detection performance exactly, the computation complexity increases rapidly as the number of sensors and sample sizes increase. To circumvent this numerical burden and gain more insights into this detection problem, we derive asymptotic Gaussian approximations to the largest eigenvalue distributions under both hypotheses. As a consequence, simple closed-form results for the false alarm and missed detection probabilities are possible. In addition, a closed-form expression for the receiver operating characteristics is derived as well.

For the largest eigenvalue λ_1 of covariance matrix $\mathbf{R}$ under $\mathbf{H_0}$, it is known that (Johansson, 2000) there exists proper centering sequence, $a_1(K, N) = (\sqrt{K} + \sqrt{N})^2$, and scaling sequence $b_1(K, N) = (\sqrt{K} + \sqrt{N})(\sqrt{\frac{1}{K}} + \sqrt{\frac{1}{N}})^{1/3}$, such that the distribution of the random variable

$$\Lambda_1 = \frac{\lambda_1 - \sigma_{cn}^2 a_1(K, N)}{\sigma_{cn}^2 b_1(K, N)}, \tag{12}$$

converges to the Tracy-Widom distribution of order two (Tracy & Widom, 1996), denoted as F_{TW2}. The convergence occurs when $K \to \infty$, $N \to \infty$ and $\frac{K}{N} \to c \in (0, 1)$. This asymptotical result provides us an approximation to the largest eigenvalue distribution for a given matrix size K and N. Namely, the CDF for the largest eigenvalue of a covariance matrix with N degrees of freedom can be approximated by a linear transform of the Tracy-Widom variable as

$$F_c \left(x \, | \sigma_{cn}^2 \right) \approx F_{TW2} \left(\frac{x - \sigma_{cn}^2 a_1(K, N)}{\sigma_{cn}^2 b_1(K, N)} \right). \tag{13}$$

The distribution function of the Tracy-Widom distribution of order two can be represented as

$$F_{TW2}(x) = \exp \left\{ - \int_x^\infty (s - x) q^2(s) ds \right\}, \tag{14}$$

where $q(s)$ is the solution to the Painlevé II differential equation $q''(s) = sq(s) + 2q^3(s)$ with boundary condition $q(s) \sim \text{Ai}(s)$ $(s \to \infty)$, where $\text{Ai}(s)$ is the Airy function. Numerically it is possible to compute the value of $F_{TW2}(x)$ for a given x by using software packages such as (Dieng, 2006; Perry et al., 2009). This facilitates efficient calculations of the approximative CDF in (13). However, equation (13) is not a closed-form approximation, since it depends on the numerical solution of (14). On the other hand, it is shown in (Anderson, 1963) that the largest eigenvalue distribution converges to a Gaussian distribution when N goes to infinity for any fixed K. Although this asymptotic result gives only a loose bound for finite-dimensional expressions, it motivates us to adopt the Gaussian approximation to the largest eigenvalue distribution. In order to obtain a closed-form Gaussian approximation we need to calculate the first two moments of λ_1, which is a non-trivial problem from the exact

distribution (6). However the asymptotic moments of λ_1 via the Tracy-Widom distribution are readily obtained. From (12), the first moment of λ_1 is

$$E[\lambda_1] = \sigma_{cn}^2(a_1(K,N) + b_1(K,N)E[\Lambda_1]), \tag{15}$$

where $E[\cdot]$ donates the expected value. The second moment of λ_1 is

$$V[\lambda_1] = (\sigma_{cn}^2 b_1(K,N))^2 V[\Lambda_1], \tag{16}$$

where $V[\cdot]$ denotes the variance. Since the distribution of Λ_1 converge to F_{TW2} as $K \to \infty$, $N \to \infty$ and $\frac{K}{N} \to c \in (0,1)$, the mean and variance of Λ_1 also converges to the ones of the Tracy-Widom variable; $E[\Lambda_1] \to E[x_{TW2}] = -1.7711$, $V[\Lambda_1] \to V[x_{TW2}] = 0.8132$. These numerical values are obtained by using (Dieng, 2006). A closed-form Gaussian approximation is obtained by fitting these two moments to the corresponding Gaussian moments. Note that by matching higher moments of the Tracy-Widow distribution to higher moments of other distributions, for example, the generalized lambda distribution (Karian & Dudewicz, 2000), we expect to achieve more accurate approximations. Finally, the largest eigenvalue distribution is approximated by a Gaussian distribution $\mathcal{N}(\mu_1, \sigma_1^2)$ with mean μ_1 and variance σ_1^2 given by $\mu_1 = \sigma_{cn}^2(a_1(K,N) + b_1(K,N)E[x_{TW2}])$ and $\sigma_1^2 = (\sigma_{cn}^2 b_1(K,N))^2 V[x_{TW2}]$ respectively. Thus the approximative CDF of λ_1 under $\mathbf{H_0}$ is

$$G_c\left(x \,|\sigma_{cn}^2\right) = \Phi\left(\frac{x - \mu_1}{\sigma_1}\right), \tag{17}$$

where $\Phi(\cdot)$ is the CDF of a standard Gaussian random variable. Note that both μ_1 and σ_1^2 are simple functions of the matrix dimensions and noise variance only. Thus the computational complexity is negligible compared with the exact distribution (6). More importantly, by using this closed-form approximation the reliance on numerical calculations from the software package (Dieng, 2006; Perry et al., 2009) is removed.

Under $\mathbf{H_1}$, the covariance matrix $\mathbf{R}$ follows the complex noncentral Wishart distribution. Simple and accurate closed-form approximation for its largest eigenvalue distribution is not available. The first order expansion of λ_1 proposed in (Jin et al., 2008) is unable to capture the detection performance since its accuracy can not be guaranteed except for a threshold around zero. In the following we propose a two-step Gaussian approximation for the λ_1 distribution under $\mathbf{H_1}$. The first step is to establish the relationship between non-central and central Wishart matrices. The results in (Tan & Gupta, 1983) showed that a non-central Wishart matrix $\mathbf{R}$ distributed as $\mathbf{R} \sim \mathcal{W}_K\left(N, \sigma_{cn}^2\mathbf{I}_K, \mathbf{MM}^H\right)$, can be well approximated by a correlated central Wishart matrix distributed as $\mathbf{R} \sim \mathcal{W}_K\left(N, \Sigma_K\right)$, where the effective correlation matrix Σ_K is given by $\Sigma_K = \sigma_{cn}^2\mathbf{I}_K + \mathbf{MM}^H/N$. Since the effective correlation matrix is an identity matrix plus a rank one matrix, the eigenvalues of Σ_K, denoted by ξ_i, can be easily determined as $\xi_1 = \sigma_{cn}^2 + \phi_1/N$, $\xi_2 = \xi_3 \ldots = \xi_K = \sigma_{cn}^2$. The second step is to approximate the largest eigenvalue distribution of a correlated central Wishart matrix by its asymptotic distribution. The results in (Baik & Silverstein, 2005) prove that the largest eigenvalue of a correlated central Wishart matrix converges to a Gaussian distribution $\mathcal{N}(\mu_2, \sigma_2^2)$ with mean $\mu_2 = N\xi_1\left(1 + \frac{K/N}{\xi_1 - 1}\right)$, and variance $\sigma_2^2 = N\xi_1^2\left(1 - \frac{K/N}{(\xi_1 - 1)^2}\right)$. The convergence occurs when $K \to \infty$, $N \to \infty$, $\frac{K}{N} \to c \in (0,1)$, and in addition ξ_1 must satisfy (Baik & Silverstein, 2005), $\xi_1 > 1 + \sqrt{K/N}$. Thus the approximative CDF of λ_1 under $\mathbf{H_1}$, denoted by $G_{nc}\left(x \,|\sigma_{cn}^2\right)$,

is represented as

$$G_{\text{nc}}\left(x \mid \sigma_{\text{cn}}^2\right) = \Phi\left(\frac{x - \mu_2}{\sigma_2}\right). \qquad (18)$$

Based on the approximative distribution of the test statistics under $\mathbf{H_0}$ (17), for a given threshold γ, the false alarm probability can be approximated by

$$P_{\text{fa}}(\gamma) \approx 1 - \Phi\left(\frac{\gamma - \mu_1}{\sigma_1}\right). \qquad (19)$$

Equivalently, for a required false alarm probability the decision threshold can be approximated by $\gamma \approx \mu_1 + \sigma_1 \Phi^{-1}(1 - P_{\text{fa}})$, where $\Phi^{-1}(\cdot)$ is the inverse of a Gaussian CDF. For a given SNR and threshold, the missed detection probability can be obtained by using the approximative distribution under $\mathbf{H_1}$ (18) as

$$P_{\text{m}}(\gamma) \approx \Phi\left(\frac{\gamma - \mu_2}{\sigma_2}\right). \qquad (20)$$

Similarly for a required missed detection probability and SNR, the approximative decision threshold is $\gamma \approx \mu_2 + \sigma_2 \Phi^{-1}(P_{\text{m}})$. Finally, by inserting this approximative threshold into (19) we obtain a closed-form approximative receiver operating characteristics for the LE detector

$$P_{\text{m}} \approx \Phi\left(\frac{\sigma_1 \Phi^{-1}(1 - P_{\text{fa}}) + \mu_1 - \mu_2}{\sigma_2}\right). \qquad (21)$$

Note that a closed-form ROC expression is not possible by using exact distributions (10) and (11). In the next section we will compare the asymptotic results with the exact distributions in terms of various detection performance metrics.

3.3 A note on computational complexity

The computational complexity discussed here refers to the on-line implementation complexity for the LE detector. If the implementation is based on look-up tables, the computational complexity is negligible when using the approximative distributions. As one can see from (17) and (18), only a 1D table (percentiles of a standard Gaussian CDF) is needed, which is applicable to any K, N and σ_{cn}^2. It can be seen from (6) and (9) that the look-up table implementation using the exact distributions is more demanding. Under $\mathbf{H_0}$ for each combination of K and N, a 1D table is needed, which is valid for any σ_{cn}^2. Moreover, under $\mathbf{H_1}$, for each combination of K and N, a 2D table is needed, which is valid for any σ_{cn}^2. The reason being that the first column of $\widehat{\mathbf{B}}$ is a function of two variables.

Since K and N may be subject to frequent changes in practice, the implementation may rely on realtime computations of the distributions instead of tabulations. In this case the operational complexity when using the exact distribution, which is mainly determined by the number of multiplications, can be shown to be upper bounded by $O(2n^3)$ for both $\mathbf{H_0}$ and $\mathbf{H_1}$ (Borwein & Borwein, 1987), where n is the number of digits needed to represent N, K, σ_{cn}^2 and the threshold γ. However, the bit-complexity may prevent the use of the exact results. Each multiplication needs to be done with a large n, which is particularly true for $\mathbf{H_1}$. For example when $K = 4$, $N = 100$ and $\sigma_{\text{cn}}^2 = 1$, by inspecting the distributions (6) and (9), it can be verified that the number of digits n equals 13 and 30 bits for $\mathbf{H_0}$ and $\mathbf{H_1}$, respectively.

4. Detection performance

In this section, several aspects regarding the detection performance are addressed. Firstly we will show the accuracy of the derived asymptotic results in characterizing the detection performance. Then we will compare the performance of the largest eigenvalue based detection to other detection methods, such as the eigenvalue ratio based detection (Penna et al., 2009B; Penna & Garello, 2010) and the energy detection. Finally we will discuss the robustness of the LE detector under noise uncertainty.

4.1 Exact versus asymptotic

The exact characterization versus the asymptotic approximation is basically a trade-off between accuracy and complexity. Here the accuracy means the degree of control in determining the performance metrics, especially the decision threshold. The complexity refers to the computational complexity in calculating various performance metrics from the test statistics distributions. When using the exact distributions (6) and (9), the false alarm probability and the missed detection probability can be determined exactly, thus we have complete control over the decision threshold. However the computational complexity in this case is non-trivial, since the exact distributions (6) and (9) involve matrix determinants with special function as entries. On the other hand, the asymptotic test statistics distributions (17) and (18) provide a trade-off between accuracy and complexity. Since both the approximative false alarm probability (19) and the approximative missed detection probability (20) are Gaussian distributions, the computational complexity in characterizing the detection performance is negligible. In Figure 1, we plot the false alarm probability as a
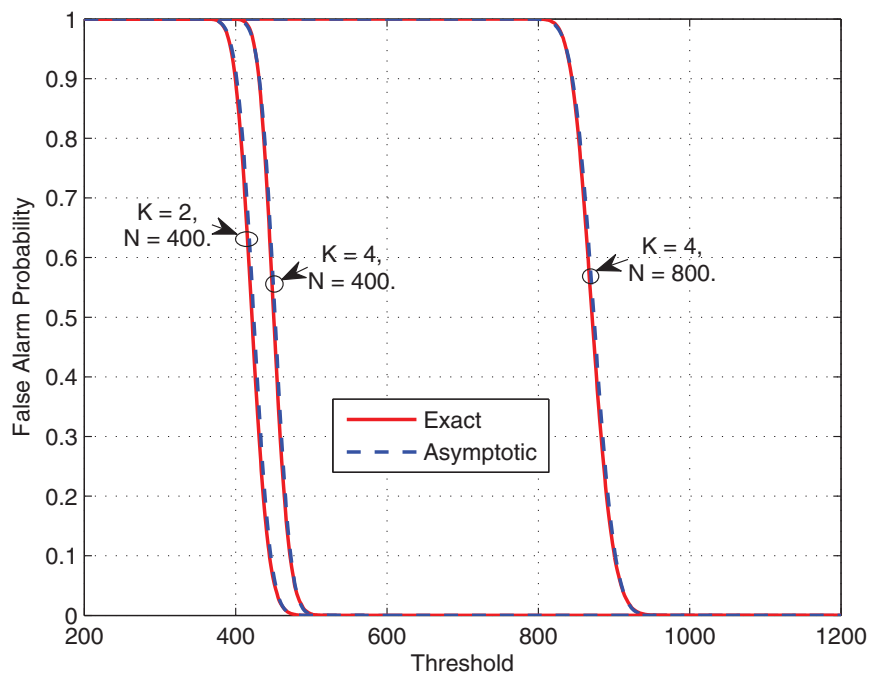
Fig. 1. False alarm probability as a function of threshold: exact v.s asymptotic.

function of the decision threshold for various K and N. The exact curves and the asymptotic curves are obtained from (10) and (19) respectively. We can see from this figure that the asymptotic approximation matches well with the exact characterization in all the parameter

settings considered. Note that the considered parameter values (K, N) are realistic in practical spectrum sensing scenarios. The number of samples N can be huge due to the high sample rate. For example, in Digital Television (DTV) signal detection problem studied in (Tawil, 2006), 100 thousand samples corresponds to only 4.65 ms sensing time. The number of receive antennas K can be safely chosen to be less or equal to eight, since nowadays it is possible to have a device with eight antennas. In Figure 2 and Figure 3, we show the missed detection
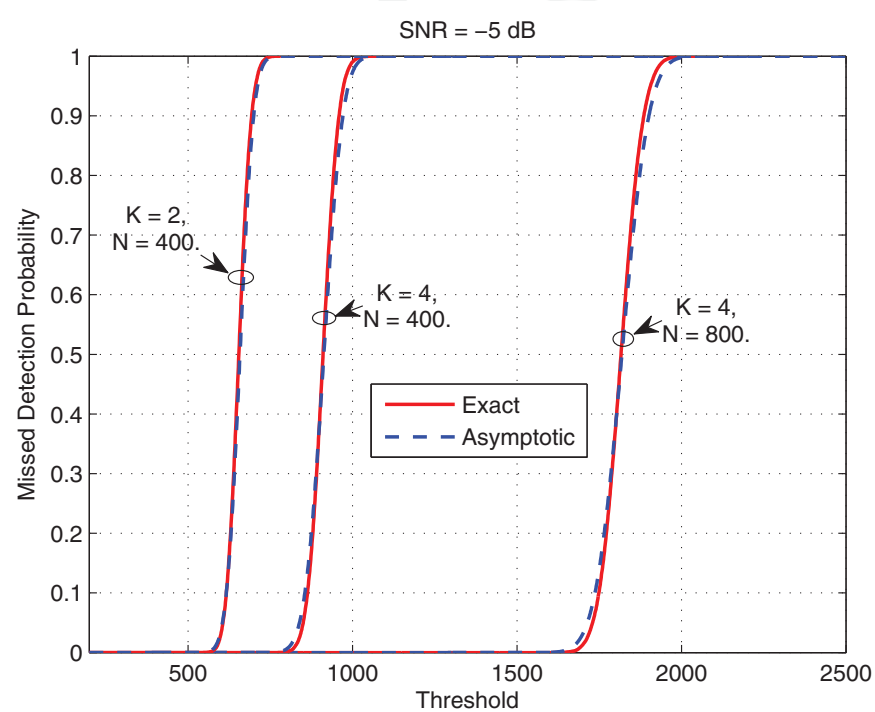
Fig. 2. Missed detection probability as a function of threshold: exact v.s asymptotic.

probability as a function of the decision threshold when SNR equals -5 dB and -10 dB respectively. The (K, N) pairs considered here are the same as in the previous figure. The exact P_m plots are obtained by using (11) and the approximative P_m plots are obtained from (20). It can be observed from these two figures that the approximation to the missed detection probability (20) is close to the exact result for different (K, N) pairs and SNR values.

4.2 Performance comparison

In general the detection performance is a function of sensing parameters, i.e., the sample size, the number of sensors and the SNR. We can compare the performances by looking at the detection probability for a fixed false alarm probability. Alternatively, the detection performance can be seen from the receiver operating characteristics curve. The ROC curve shows the achieved probability of missed detection as a function of the target false alarm probability. Thus the ROC curve illustrates the overall detection performance for a given detector.

In this subsection, we will compare the LE detector with the classical energy detector (Digham et al., 2003) and the recently proposed eigenvalue ratio (condition number) based detector (Penna et al., 2009A;B; Penna & Garello, 2010) by means of the ROC curves. Specifically, we show how the different sensing parameters (number of sensors, sample size and SNR) affect the detection performance. Here we investigate the case when the noise variance is known
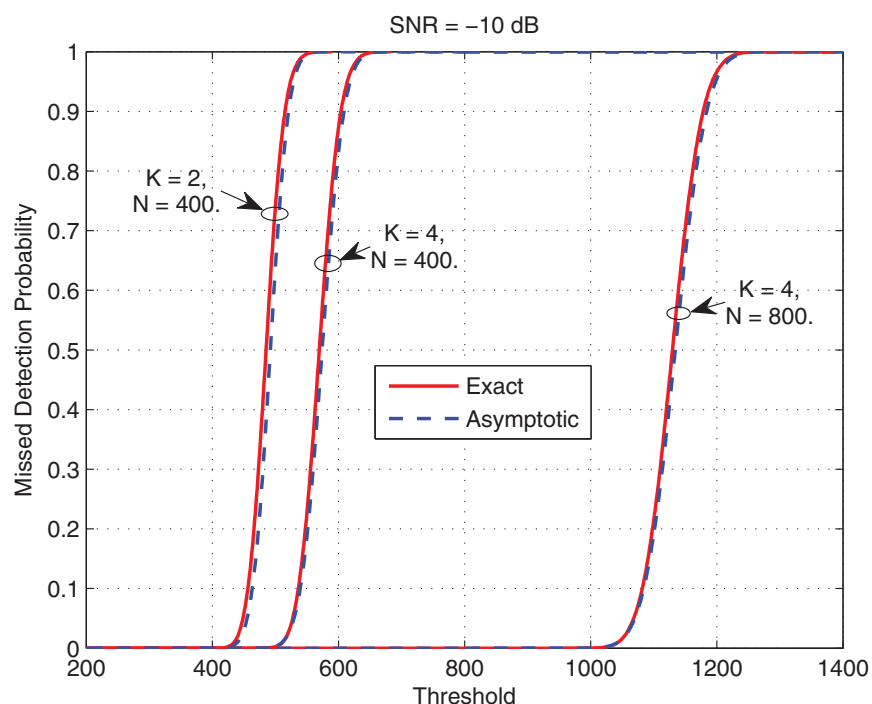
Fig. 3. Missed detection probability as a function of threshold: exact v.s asymptotic.

exactly. The case when there is uncertainty about the noise variance estimates is studied in the next subsection.

The cooperative energy detector will collaborate in the same way as the LE detector in that the decision statistics is a function of the collaboratively formed the received data matrix $\mathbf{Y}$ (1). In the case of the energy detector the test statistics is the norm of received data matrix $\mathbf{Y}$, for example, the Frobenius norm $||\mathbf{Y}||_F^2$. The decision rule is to choose $\mathbf{H_0}$ when $||\mathbf{Y}||_F^2 \leq \gamma$ and choose $\mathbf{H_1}$ when $||\mathbf{Y}||_F^2 > \gamma$. Under $\mathbf{H_0}$, the test statistics $||\mathbf{Y}||_F^2$ follows the central Chi-square distribution with 2KN degrees of freedom (Digham et al., 2003; Proakis, 2001). Under $\mathbf{H_1}$, the test statistics follows the non-central Chi-square distribution with 2KN degree of freedom. In addition to the LE detector, another possible eigenvalue based detector is the eigenvalue ratio based detector. With the test statistics is $T_{\mathrm{ER}} = \lambda_1 / \lambda_K$. Asymptotic approximations of T_{ER} distribution under both hypotheses are studied in (Penna et al., 2009B; Penna & Garello, 2010) and the exact distribution of T_{ER} under $\mathbf{H_0}$ is studied in (Penna et al., 2009A). It can be shown that the test statistics of the ER detector does not depend on noise variance asymptotically. Therefore the ER detector is immune to the noise uncertainty problem.

Without loss of generality, we set variance of the complex noise to 1 ($\sigma_{\mathrm{cn}}^2 = 1$). In the following figures, we will compare the detection performance of LE detector with that of the energy detector and the ER detector. In Figure 4, we consider a case where the number of sensors (receive antennas) is 4, the sample size is 600 per sensor and the SNR is -10 dB. For LE detector, the exact ROC curve is obtained from (10) and (11) while the approximative ROC is drawn by using (21). For the ER detector, the ROC curve is obtained by simulation. From this figure we can see that the LE detector uniformly outperforms both the energy detector and the ER detector since its probability of missed detection is lower for all false alarm probabilities. Moreover we observe that the asymptotic approximative ROC represents the detection performance rather accurately. In Figure 5, we consider a different sensing
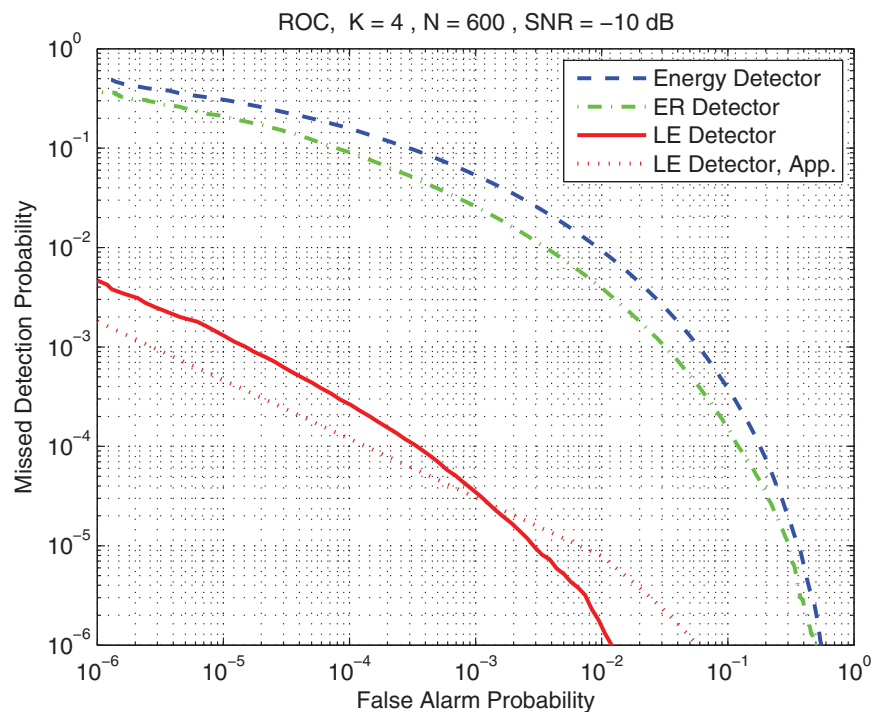
Fig. 4. Receiver operating characteristics: $K = 4$, $N = 600$, $\text{SNR} = -10$ dB.
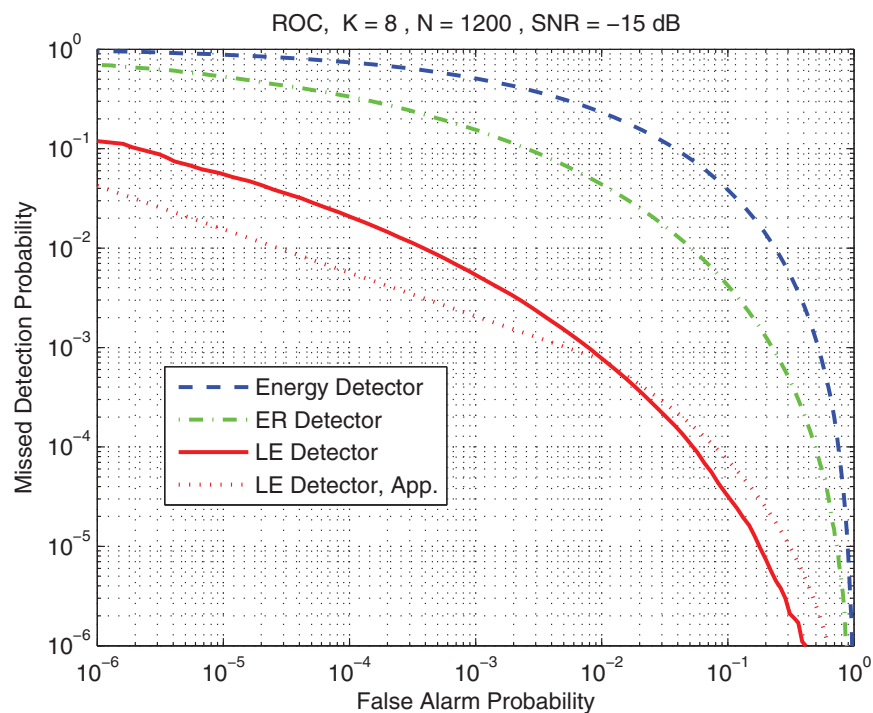

Fig. 5. Receiver operating characteristics: $K = 8$, $N = 1200$, $\text{SNR} = -15$ dB.

parameter setting where the number of sensor is 8 with 1200 samples per sensor and SNR -15 dB. In this setting, we again observe that the LE detector performs best among the detectors considered and the loss in characterizing the performance by the approximate ROC is tolerable.

The superior performance of the LE detector over the energy detector can be understood as follows. For cooperative energy detection, the test statistics $||\mathbf{Y}||_F^2$, by definition, equals $||\mathbf{Y}||_F^2 = \text{tr}\{\mathbf{Y}\mathbf{Y}^H\} = \text{tr}\{\mathbf{R}\} = \sum_{i=1}^{K} \lambda_i$, where λ_i is the ith eigenvalue of the received covariance matrix $\mathbf{R}$. Therefore, the test statistics of the energy detector blindly sums up all the K eigenvalues from the covariance matrix $\mathbf{R}$. On the other hand, for the LE detection the test statistics only involves λ_1. In other words, the LE detector will intentionally pick up only the largest eigenvalue as decision statistics. This is an optimal statistical test when there is only one primary user present (matrix $\mathbf{M}$ being rank one) (Roy, 1953). Recall also the implication from Table 1 that blindly adding more eigenvalues as test statistics is unnecessary. When summing all eigenvalues one obtains a more heavy-tailed distribution than the largest eigenvalue distribution. This-heavy tailed distribution will lead to worse detection performance of the energy detector, which is the main motivation behind the LE detector.

4.3 Noise uncertainty analysis

In the analysis done so far we assume the noise variance is known exactly. This is an ideal scenario considering that in any practical system modeling of noise uncertainty is unavoidable. It is especially true for detection problems in CR networks, where robustness to noise uncertainty is a fundamental performance metric (Tandra & Sahai, 2005; 2008). Uncertainty in noise variance may arise due to noise estimation error in the receiver or noise variations during the sensing time or interference caused by other primary users. Note that noise uncertainty analysis may be generalized to incorporate interference uncertainty as well (Zeng et al., 2009).

We consider a situation where there is uncertainty about the noise variance. Let μ be the value in dB of the noise uncertainty. Then the noise power will fall in the interval $\Omega = [\sigma_{\text{cn}}^2/\rho, \rho\sigma_{\text{cn}}^2]$, where $\rho = 10^{\mu/10}$. Naturally, as the uncertainty μ increases the interval that the noise power could fall into will be larger. We would like to see the worst case of performance degradation due to this uncertainty. Thus we need to check all the possible noise power from the interval Ω such that the PDFs under both hypotheses will overlap most. As a result of which, we have the worst case performance for a given uncertainty level μ. Due to the monotonic tails of the largest eigenvalue distributions (6), (9) the noise variance under $\mathbf{H_0}$ is now $\rho\sigma_{\text{cn}}^2$ and the corresponding distribution becomes

$$F_{\text{c}}\left(x \,|\rho\sigma_{\text{cn}}^2\right) = |\det\widehat{\mathbf{A}}|, \qquad (22)$$

with $\widehat{\mathbf{A}}_{i,j} = \binom{N-j+i-1}{i-1}\gamma_R(N+i-j, \frac{x}{\rho\sigma_{\text{cn}}^2})$. Similarly, in order to obtain worst case performance, the noise variance under $\mathbf{H_1}$ has to be $\sigma_{\text{cn}}^2/\rho$. The resulting distribution becomes

$$F_{\text{nc}}\left(x \,|\frac{\sigma_{\text{cn}}^2}{\rho}\right) = |\det\widehat{\mathbf{B}}|, \qquad (23)$$

with elements in the first column $\widehat{\mathbf{B}}_{i,1} = \frac{\Gamma(K)}{(N-K)\Gamma(N-i)}\int_0^{\rho x/\sigma_{\text{cn}}^2}\beta^{N-i}\,\text{e}^{-\beta}\,{}_0F_1\left(N-K+1; \frac{\rho\phi_1\beta}{\sigma_{\text{cn}}^2}\right)\text{d}\beta$ and in the other $K-1$ columns $\widehat{\mathbf{B}}_{i,j} = \binom{N-i+j-2}{j-1}\gamma_R(N-i+j-1, \frac{\rho x}{\sigma_{\text{cn}}^2})$, $j = 2,\ldots,N$. Notice that in the case of no noise uncertainty ($\rho \to 1$), the distributions (22) and (23) become (6) and (9) respectively. One example to illustrate the effect of noise uncertainty on the LE detector is
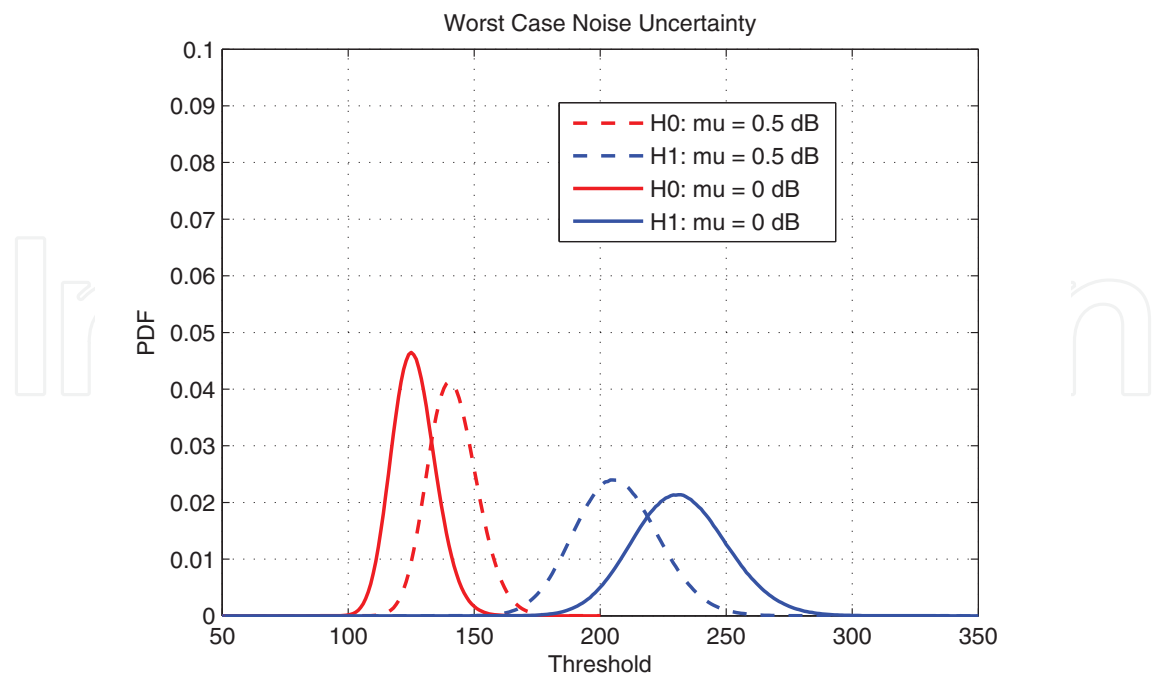
Fig. 6. Impact of worst case noise uncertainty: $K = 4$, $N = 100$, SNR $= -5$ dB, $\mu = 0.5$ dB.

presented in Figure 6, where $K = 4$, $N = 100$, SNR $= -5$ dB. We choose the noise variance $\sigma_{cn}^2 = 1$ for the case of no noise uncertainty and the uncertainty level $\mu = 0.5$ dB when considering noise uncertainty. Therefore in the worst case scenario the noise variance is 1.122 under $\mathbf{H_0}$ and is 0.891 under $\mathbf{H_1}$. In Figure 6 we plot the PDFs of the test statistics with and without noise uncertainty. We observe that for the case of noise uncertainty, we indeed obtain the worst case of distributions where the curves overlap most. Intuitively, this corresponds to the situation that the two hypotheses are most difficult to distinguish when noise uncertainty exists.

Similarly, for a given uncertainty level μ the worst case approximative test statistics distribution under $\mathbf{H_0}$ is

$$G_c \left(x \, | \rho \sigma_{cn}^2 \right), \tag{24}$$

and under $\mathbf{H_1}$ is

$$G_{nc} \left(x \, | \frac{\sigma_{cn}^2}{\rho} \right). \tag{25}$$

In the following figures we will first show the impact of the noise uncertainty on both the false alarm probability and the missed detection probability of the LE detector. In the meanwhile we will illustrate the accuracy of the approximative test statistics distributions under noise uncertainty. Then we will compare the detection performance of the LE detector with that of the energy detector and the ER detector in the case of noise uncertainty. In Figure 7, we show the false alarm probability of the LE detector as a function of the decision threshold for various (K, N) pairs under noise uncertainty. We assume to have 0.4 dB uncertainty in the noise variance. The exact curves and the asymptotic curves are obtained by using (22) and (24) respectively. Comparing this figure with Figure 1 we see that in the case of noise uncertainty the false alarm probability will increase for any given threshold and any (K, N) pairs considered. We can also observe from this figure that the asymptotic approximation
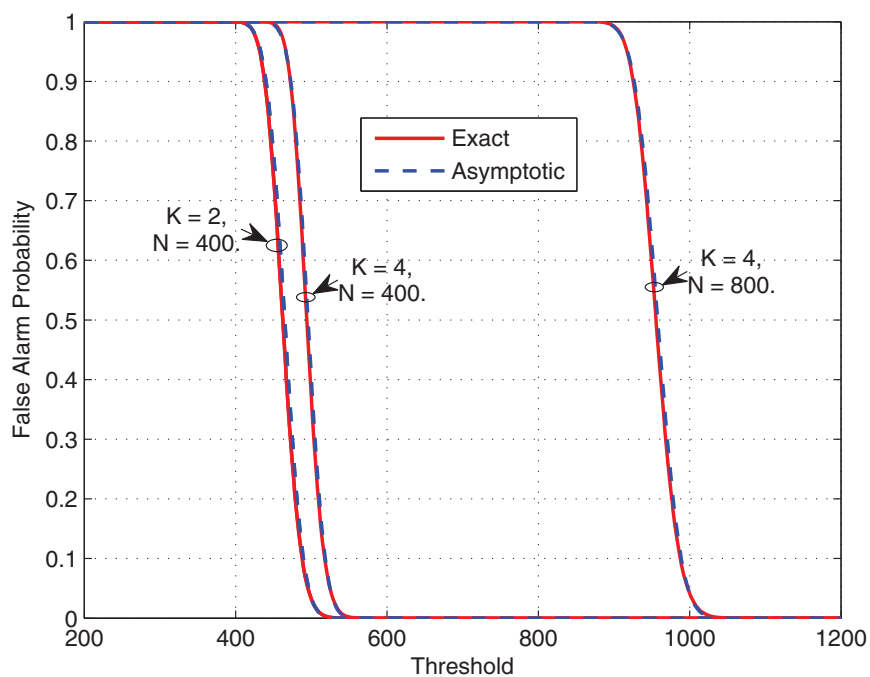
Fig. 7. False alarm probability under noise uncertainty, $\mu = 0.4$ dB: exact v.s asymptotic.

matches well with the exact characterization under noise uncertainty.   In Figure 8 and
Figure 9, we plot the missed detection probability as a function of the decision threshold
when SNR equals -5 dB and -10 dB with 0.4 dB uncertainty in the noise variance. The
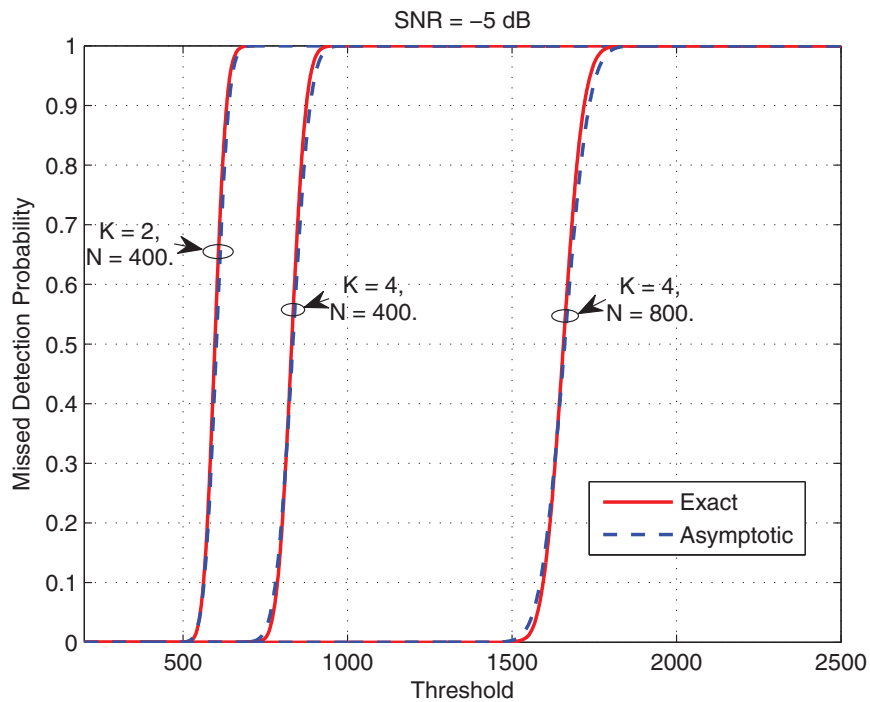exact P_m plots are obtained by using (23) and the approximative P_m plots are obtained

Fig. 8. Missed detection probability under noise uncertainty, $\mu = 0.4$ dB: exact v.s asymptotic.
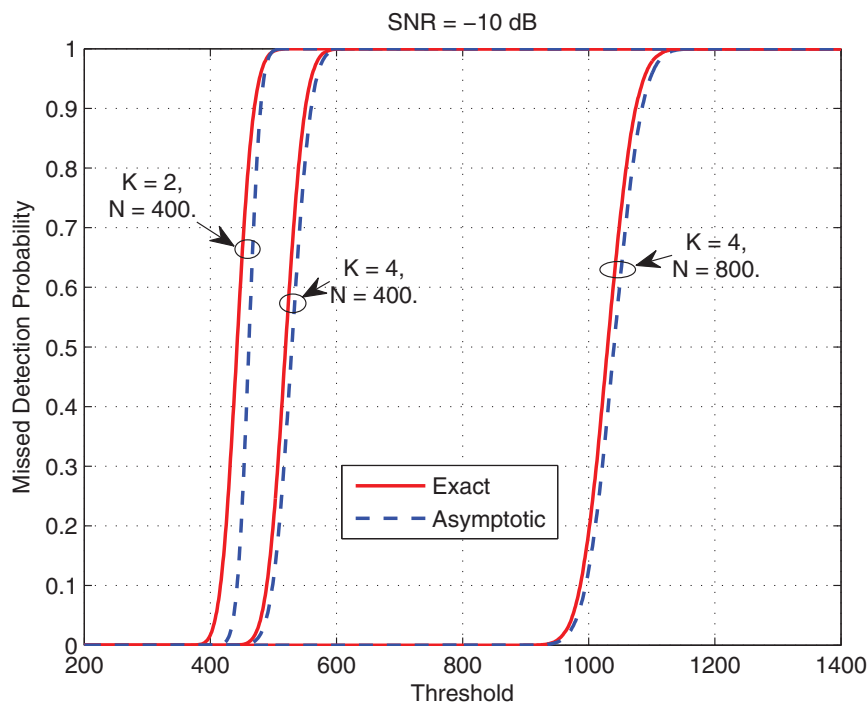
Fig. 9. Missed detection probability under noise uncertainty, $\mu = 0.4$ dB: exact v.s asymptotic.

from (25). By comparing these two figures with Figure 2 and Figure 3 respectively, it can be observed that in the case of noise uncertainty the missed detection probability will also increase for any given threshold and any (K, N) pairs considered. Therefore, we indeed obtain the worst case performance due to noise uncertainty where both the false alarm and missed detection probabilities increase for any given threshold. It can be also observed from these two figures that the asymptotic distribution of the missed detection probability provides a useful approximation for finite size (K, N) pairs. In Figure 10 we compare the impact of noise uncertainty of the LE detector with that of the energy detector and the ER detector by means of the ROC plot. The sensing parameters here are the same as in Figure 4 except that there is now 0.2 dB uncertainty in the noise variance. By comparing this figure with Figure 4, we can see that the ER detector performs better than the LE detector and the energy detector in the case of noise uncertainty. The reason is that the test statistics of the ER detector is not a function of the noise variance, thus its performance will not degrade regardless of the degree of noise uncertainty. On the other hand, the test statistics of both the LE detector and the energy detector depend on the noise variance, thus their detection performances rely on accurate estimation of the noise variance. However, we can observe that the performance degradation is much more severe for the energy detector than that of the LE detector. At $\mu = 0.2$ dB the detection performance of the LE detector and the ER detector are on the same level comparable, but the detection performance of the energy detection becomes too poor to be useful. We also observe that the implementation complexity and accuracy tradeoff reflected by the exact and approximate ROCs is affordable in practice. Finally, in Figure 11 we consider the same sensing parameter setting as in Figure 5 with the exception that we now have 0.2 dB uncertainty in the noise variance. By comparing this figure with Figure 5, we again observe that the impact of noise uncertainty on the ER detector is negligible. However, the energy detector fails in this case with the false alarm probability and the missed detection probability approaching 1. Although the LE detector still works in the case, the performance degradation
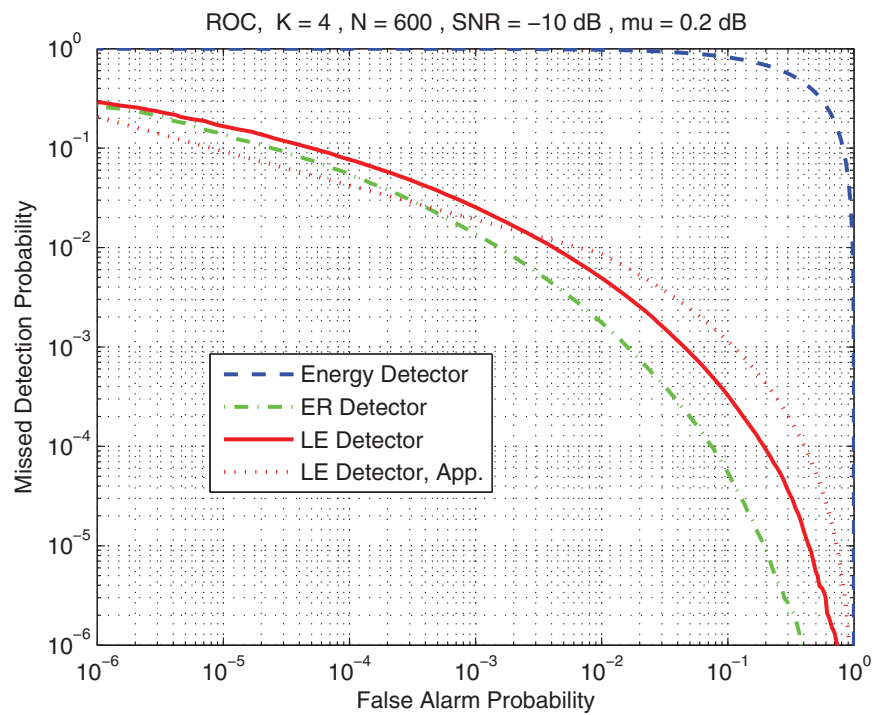
Fig. 10. Receiver operating characteristics under noise uncertainty: $K = 4$, $N = 600$, SNR $= -10$ dB, $\mu = 0.2$ dB.
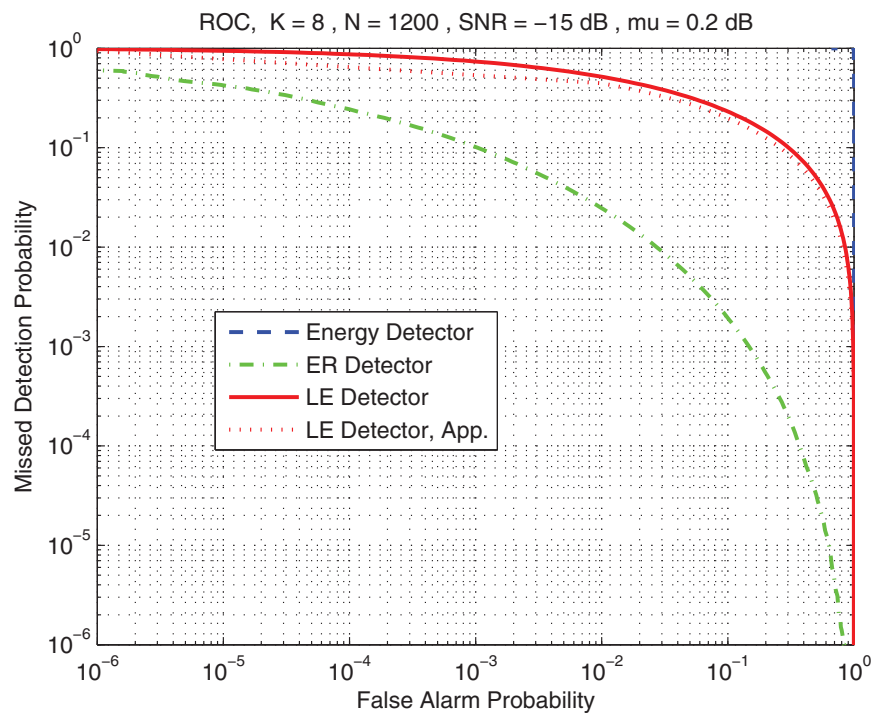

Fig. 11. Receiver operating characteristics under noise uncertainty: $K = 8$, $N = 1200$, SNR $= -15$ dB, $\mu = 0.2$ dB.

is non-trivial. We can see also that in this case the approximate ROC is able to capture the detection performance almost exactly.

5. Conclusion

In this chapter, we perform both non-asymptotic and asymptotic analysis on the performance of the largest eigenvalue based detection. Analytical formulae have been derived for various performance metrics in realistic spectrum sensing scenarios. It has been shown that the LE detector is more efficient than the energy detector and the ER detector in terms of sample size, number of sensors and SNR requirement. Our analytical framework has also been applied to investigate the detection performance in the presence of noise uncertainty, where we conclude that the superiors performance of the LE detector relies on the accurate estimation on the noise power. From implementation perspective, we studied the computational complexity and accuracy tradeoff which is resolved by the derived tight approximate ROC.

6. References

Anderson, T. W. (1963). Asymptotic theory for principal component analysis. *Ann. Math. Statist.,* 34, 122-148, 1963.

Baik, J. & Silverstein, J. (2005). Eigenvalues of large sample covariance matrices of spiked population models. *Journal of Multivariate Analysis,* 97, pp. 1382-1408, 2006.

Borwein, J. & Borwein, P. (1987). *Pi and the AGM: A Study in Analytic Number Theory and Computational Complexity*, John Wiley, 1987.

Dieng, M. (2006). RMLab, a MATLAB package for computing Tracy-Widom distributions and simulating random matrices. http://math.arizona.edu/ momar/research.htm, 2006.

Digham, F. F., Alouini, M. & Simon, M. K. (2003). On the energy detection of unknown signals over fading channels. *IEEE International Conference on Communications,* May 2003.

Dighe, P. A., Mallik, R. K. & Jamuar, S. R. (2003). Analysis of trasmit-receive diversity in Rayleigh fading. *IEEE Tran. Commun.,* vol. 51, no. 4, pp. 694-703, Apr. 2003.

Gardner, W. A. (1991). Exploitation of spectral redundancy in cyclostationary signals. *IEEE Sig. Proc. Mag.,* vol. 8, pp. 14-36, 1991.

Gupta, A. K. & Nagar, D. K. (2000). *Matrix Variate Distributions.* CRC Press, 2000.

James, A.T. (1964). Distributions of matrix variates and latent roots derived from normal samples. *Ann. Inst. Statist. Math.,* 35, 475-501, 1964.

Jin, S., McKay, M. R., Gao, X. & Collings I. B. (2008). MIMO multichannel beamforming: SER and outage using new eigenvalue distributions of complex noncentral Wishart matrices. *IEEE Tran. Commun.,* vol. 56, no. 3, pp. 424-434, Mar. 2008.

Johansson, K. (2000). Shape fluctuations and random matrices. *Comm. Math. Phys.,* 209:437-476, 2000.

Kang, M. & Alouini, M. S. (2003). Largest eigenvalue of complex wishart matrices and performance analysis of MIMO MRC systems. *IEEE J. Selec. Areas Commun.,* vol. 21, no. 3, pp. 418-426, Apr. 2003.

Karian, Z. A. & Dudewicz, E. J. (2000). *Fitting Statistical Distributions: The Generalized Lambda Distribution and Generalized Bootstrap Methods.* Chapman and Hall/CRC, 2000.

Kay, S. M. (1993). *Fundamentals of Statistical Signal Processing: Estimation Theory.* Englewood Cliffs, NJ: Prentice-Hall, 1993.

Khatri, C. G. (1964). Distribution of the largest or the smallest characteristic root under null hyperthesis concerning complex multivariate normal populations. *Ann. Math. Stat.,* 35, 1807-1810, 1964.

Kritchman, S. & Nadler, B. (2009). Non-parametric detections of the number of signals: hypothesis testing and random matrix theory. *IEEE Trans. Sig. Proc.,* vol. 57, no. 10, pp. 3930-3941, 2009.

Penna, F., Garello, R., Figlioli, D., & Spirito, M. A. (2009). Exact non-asymptotic threshold for eigenvalue-based spectrum sensing. *IEEE International Conference on Cognitive Radio Oriented Wireless Networks and Communications,* Jun. 2009.

Penna, F., Garello, R., & Spirito, M. A. (2009). Cooperative spectrum sensing based on the limiting eigenvalue ratio distribution in Wishart matrices. *IEEE Comm. Letters,* vol. 13, issue 7, pp. 507-509, Jul. 2009.

Penna, F. & Garello, R. (2010). Eigenvalue ratio detection: identifiability and missed-detection probability. *arXiv: 0907.1523.*

Perry, P. O., Johnstone, I. M., Ma, Z. & Shahram, M. (2009). RMTstat: Distributions and Statistics from Random Matrix Theory. 2009, R software package version 0.1.

Proakis, J. G. (2001). *Digital Communications,* Boston, MA: McGraw-Hill, 4th edition, 2001.

Roy, S. N. (1953). On a heuristic method of test construction and its use in multivariate analysis. *Ann. Math. Stat.,* vol. 24, no. 2, pp. 220-238, 1953.

Ruttik, K., Koufos, K. & Jantti, R. (2009). Spectrum sensing with multiple antennas. *IEEE International Conference on Systems, Man, and Cybernetics,* Oct. 2009.

Sahai, A. & Cabric, D. (2005). Spectrum sensing: fundamental limits and practical challenges. *IEEE International Symposium on New Frontiers in Dynamic Spectrum Access Network,* Nov. 2005.

Tan, W. Y. & Gupta, R. P. (1983). On approximating the non-central Wishart distribution with Wishart distribution. *Commun. Stat. Theory Method,* vol. 12, no. 22, pp. 2589-2600, 1983.

Tandra, R. & Sahai, A. (2005). Fundamental limits on detection in low SNR under noise uncertainty. *WirelessCom.,* Jun. 2005.

Tandra, R. & Sahai, A. (2008). SNR walls for signal detection. *IEEE J. Select. Topic in Sig. Proc.,* vol. 2, no. 1, Feb. 2008.

Tawil, V. (2006). 51 captured DTV signal. May 2006, http://grouper.ieee.org/groups/802/22/.

Tracy, C. & Widom, H. (1996). On orthogonal and symplectic matrix ensembles. *Comm. Math. Phys,* vol.177, pp.727-754, 1996.

Wei, L. & Tirkkonen, O. (2009). Cooperative spectrum sensing of OFDM signals using largest eigenvalue distributions. *IEEE International Symposium on Personal, Indoor and Mobile Radio Communications,* Sep. 2009.

Zeng, Y., Koh, C. L. & Liang, Y.-C. (2008). Maximum eigenvalue detection: theory and application. *IEEE International Conference on Communications,* May 2008.

Zeng, Y. & Liang, Y.-C. (2008). Eigenvalue based spectrum sensing algorithms for cognitive radio. *IEEE Tran. Commun.,* vol. 57, no. 6, pp.1784-1793, Jun. 2009.

Zeng, Y., Liang, Y.-C. & Peh, Edward C. Y. (2009). Reliability of spectrum sensing under noise and interference uncertainty. *IEEE International Workshop on the Network of the Future,* 2009.

Foundation of Cognitive Radio Systems

Edited by Prof. Samuel Cheng

The fast user growth in wireless communications has created significant demands for new wireless services in both the licensed and unlicensed frequency spectra. Since many spectra are not fully utilized most of the time, cognitive radio, as a form of spectrum reuse, can be an effective means to significantly boost communications resources. Since its introduction in late last century, cognitive radio has attracted wide attention from academics to industry. Despite the efforts from the research community, there are still many issues of applying it in practice. This books is an attempt to cover some of the open issues across the area and introduce some insight to many of the problems. It contains thirteen chapters written by experts across the globe covering topics including spectrum sensing fundamental, cooperative sensing, spectrum management, and interaction among users.

How to reference

In order to correctly reference this scholarly work, feel free to copy and paste the following:

INTECH
open science | open minds